Molecular Biology of the Cell
Vol. 6, 1367–1380, October 1995

Computer Analysis of the Binding Reactions Leading to a Transmembrane Receptor-linked Multiprotein Complex Involved in Bacterial Chemotaxis

Dennis Bray*† and Robert B. Bourret‡

†Department of Zoology, University of Cambridge, Cambridge CB2 3EJ, United Kingdom; and
‡Department of Microbiology and Immunology, University of North Carolina, Chapel Hill, North Carolina 27599-7290

Submitted May 15, 1995; Accepted August 1, 1995
Monitoring Editor: Lucy Shapiro

The chemotactic response of bacteria is mediated by complexes containing two molecules each of a transmembrane receptor and the intracellular signaling proteins CheA and CheW. Mutants in which one or the other of the proteins of this complex are absent, inactive, or expressed at elevated amounts show altered chemotactic behavior and the phenotypes are difficult to interpret for some overexpression mutants. We have examined the possibility that these unexpected phenotypes might arise from the binding steps that lead to active complex formation. A limited genetic algorithm was used to search for sets of binding reactions and associated binding constants expected to give mutant phenotypes in accord with experimental data. Different sets of binding equilibria and different assumptions about the activity of particular receptor complexes were tried. Computer analysis demonstrated that it is possible to obtain sets of binding equilibria consistent with the observed phenotypes and provided a simple explanation for these phenotypes in terms of the distribution of active and inactive complexes formed under various conditions. Optimization methods of this kind offer a unique way to analyze reactions taking place inside living cells based on behavioral data.

INTRODUCTION

The signal transduction network that controls bacterial chemotaxis employs a cascade of transient protein phosphorylation and dephosphorylation reactions to transmit information about the external environment to the flagellar motor (for reviews see Bourret *et al.*, 1991; Stock *et al.*, 1991). As is the case for many eukaryotic signaling pathways (see for example Pawson and Schlessinger, 1993), the intracellular signals in bacterial chemotaxis originate in transmembrane receptor-linked multiprotein complexes that form on the inner face of the plasma membrane (Gegner *et al.*, 1992; Maddock and Shapiro, 1993; Schuster *et al.*, 1993). The complex responsible for chemotaxis to aspartate, in particular, contains the dimeric aspartate-binding receptor Tar (TT)[1] (Milligan and Koshland, 1988) and two cytoplasmic proteins, CheW (W), which is a monomer (Gegner and Dahlquist, 1991), and CheA (AA), which is a dimer under most conditions (Gegner and Dahlquist, 1991). The complex is believed to have the composition TTWWAA (Gegner *et al.*, 1992).

The ligand binding state of TT controls the autophosphorylation rate of AA in the complex (Borkovich *et al.*, 1989; Borkovich and Simon, 1990; Ninfa *et al.*, 1991) and hence the flow of phosphoryl groups through the signal transduction pathway (Figure 1). The pathway branches with the transfer of phosphoryl groups from CheA-P to CheY (Y) and CheB (B) (Hess *et al.*, 1988b; Wylie *et al.*, 1988). Y can also autophosphorylate using small molecule phosphodonors such

* Corresponding author.

[1] Abbreviations used: AA, CheA dimer; B, CheB; Bp, phosphorylated CheB; CCW, counterclockwise; CW, clockwise; R, CheR; TT, Tar dimer; W, CheW monomer; Y, CheY; Yp, phosphorylated CheY; Z, CheZ.

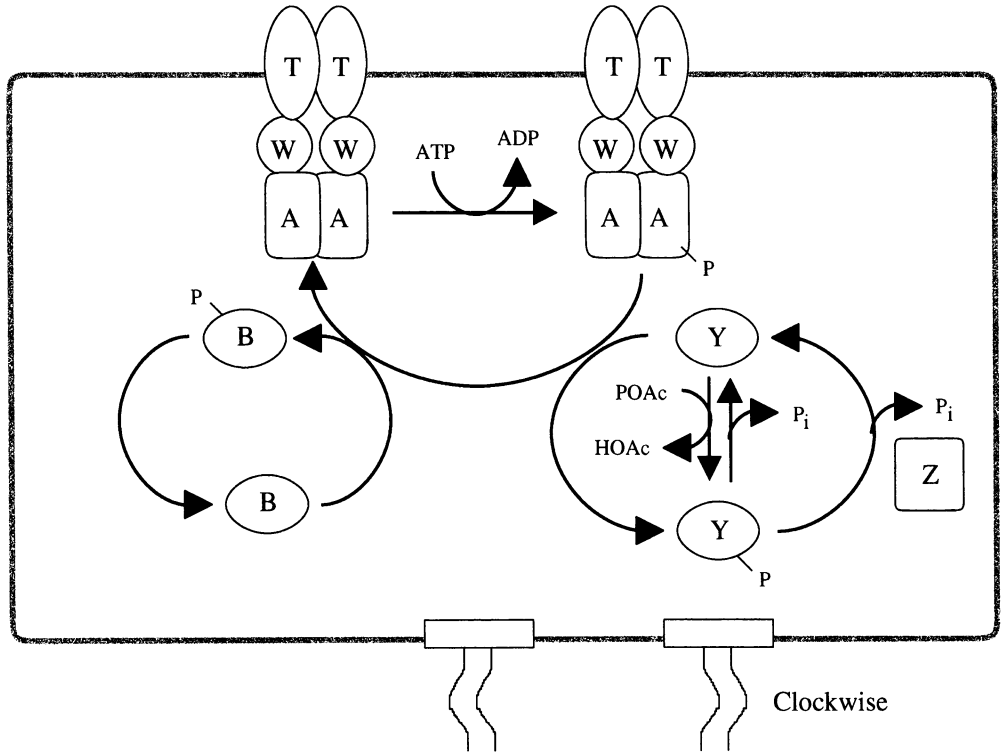

Figure 1. Schematic view of the receptor-associated complex and its role in the transduction of chemotactic signals. The chemotactic stimulus, in this case the attractant aspartate or the repellent nickel ions, bind specifically to the transmembrane receptor Tar (TT) causing a conformation change. This is transmitted across the plasma membrane to a complex of proteins including CheW (W) and CheA dimers (AA). The "signal" or conformational change causes a change in the rate of AA autophosphorylation; AA autophosphorylation increases in response to repellents and decreases in response to attractants. The phosphoryl group is transferred from the protein complex to CheY (Y) or CheB (B). Phosphorylated CheY then diffuses to the flagellar motor and changes the direction of its rotation. In this way, the detection of chemotactic attractant or repellent produces a change in swimming behavior of the bacterium. Note that other complexes formed from TT, W, and/or AA presumably exist and participate in various reactions as catalogued in Table 1 but are not shown here. The methylation reactions of the adaptation pathway catalyzed by CheR and CheB are not included in the simulation and are also not shown here. The simulation includes the possibility of ligand binding to all complexes that include the receptor TT, but the effects of ligand binding are not explored in this manuscript.

as acetyl phosphate (Lukat *et al.*, 1992). In the excitation pathway, phosphorylated CheY (Yp) binds to the FliM protein in the switch at the base of the flagellar motor to change flagellar rotation from the default counterclockwise (CCW) direction to clockwise (CW) and thus control bacterial swimming behavior (Barak and Eisenbach, 1992; Welch *et al.*, 1993, 1994). In the adaptation pathway, phosphorylated CheB (Bp) adjusts receptor methylation state in a phosphorylation-dependent manner to further regulate receptor signaling strength (Lupas and Stock, 1989; Borkovich *et al.*, 1992). The signaling species turn over rapidly to accurately represent changing external conditions. Yp and Bp spontaneously autodephosphorylate (Hess *et al.*, 1988b; Wylie *et al.*, 1988), and dephosphorylation of Yp is further stimulated by the CheZ (Z) protein (Hess *et al.*, 1988a).

Mutant bacteria in which TT, W, and AA, separately or together, are removed or expressed in higher than normal amounts have previously been isolated and their swimming behavior has been characterized (Parkinson, 1978; Stewart *et al.*, 1988; Liu and Parkinson, 1989; Sanders *et al.*, 1989). Biochemical studies provide information on some of the crucial binding steps in formation of the active complex (Gegner and Dahlquist, 1991; McNally and Matsumura, 1991; Gegner *et al.*, 1992; Bourret *et al.*, 1993; Schuster *et al.*, 1993; Swanson *et al*, 1993a,b; Wolfe *et al.*, 1994) but the pathway of its formation and the dissociation constants of intermediate complexes are not known.

We have used a computer-based approach to try to deduce the binding steps involved in the formation of TTWWAA from TT, W, and AA. Briefly, the procedure entailed testing the performance of different networks by numerical integration for both wild-type and mutant genotypes and changing the dissociation constants until the performance corresponded with experimental data. In this way we obtained sets of binding steps compatible with the phenotype of mutants with altered levels of TT, W, or AA. Note that *Escherichia coli* and *Salmonella typhimurium* each contain multiple transmembrane receptor species (reviewed in Hazelbauer *et al.*, 1990) but for simplicity, we have considered the case where TT is the only type of receptor present. Thus changing levels of TT in the model corresponds to changing amounts of the entire receptor population in a real bacterium. The mutants chosen to provide boundary conditions for the optimization procedure included strains with overexpressed TT or W, which give the same swimming behavior as those in which TT or W have been deleted. This seemingly paradoxical result has been suggested

to arise from an accumulation of inactive complexes (Gegner *et al.*, 1992; Swanson *et al.*, 1993a). Some of the networks tested included the complexes TTAA and TTWAA, which have not been fully tested experimentally. The possibility that TTWAA has full autophosphorylation activity comparable to TTWWAA was also examined.

MATERIALS AND METHODS

Formation of the active complex TTWWAA is not affected by binding of ligand to receptor, nor by AA autophosphorylation (Gegner *et al.*, 1992). We were therefore able to model the binding interactions leading to formation of this complex separately from the rapid signaling changes occurring with ligand binding. Simulation of the response of a bacterium with a specific genotype entailed two steps. First, binding interactions between TT, W, and AA and their oligomeric complexes were allowed to come to equilibrium (representing the state of a bacterium before an experiment to measure its chemotactic performance). Then the concentration of TTWWAA produced by this set of binding interactions was used to predict the unstimulated swimming behavior of the bacterium using the computer-based simulation of the phosphorylation cascade described previously (Bray *et al.*, 1993).

Binding Interactions Leading to TTWWAA

Each network of binding interactions between TT, W, AA, and their complexes was tested to see if it could produce the desired steady state concentrations of TTWWAA for a range of genotypes. Testing entailed an optimization process in which K_d values were varied until the absolute difference between simulated TTWWAA concentrations and target TTWWAA concentrations–the "cost" value"–reached an acceptably small value. Various optimization procedures were examined, including variants of the Simplex and Simulated Annealing methods (Press *et al.*, 1992). The method found empirically to generate solutions with the least expenditure of CPU time was a limited genetic algorithm method used previously to simulate the evolution of a small network of cell signaling proteins (Bray and Lay, 1994a). In this procedure, random "mutational" changes are made in the dissociation constants of each binding step, each set of changes being followed by a selection step. Mutations were simulated by a series of random numbers between 0 and 1, generated by the routine *ran1* described by Press *et al.* (1992). These numbers were used to first select one of the dissociation (off) rates of the network, and second, to specify a factor (which ranged linearly from 0.6–1.4) by which this rate was to be multiplied. The dissociation constant of this binding step was then deduced using the relation:

$$Kd = \frac{off\ rate}{on\ rate}$$

using a constant value for the on rate, as detailed below.

A starting network, characterized by a set of initial dissociation constants, was allowed to produce "offspring" networks by an alternating sequence of groups of five mutations each followed by a selection step. At each mutation, the dissociation rate (off rate) of the binding step was multiplied by the factor:

$$(ran + 0.5)^p$$

where ran is a random number between 0 and 1, and p changed linearly from 3.0 to 1.3 as the optimization progresses. Networks were subjected to 300 sequential selection steps in this fashion and the network closest to the target was stored as an "isolate." Five independent isolates were collected from each starting network and the one with the lowest cost was then used as a founder network for another series of mutations. The entire process was repeated for a total of three rounds and the K_d values of the network with the lowest overall cost were recorded. The same optimization procedure, starting with different sets of initial K_d values, was then allowed to run automatically for a period of time, sometimes in excess of a week or more, and the solutions obtained were then analyzed as described in this paper.

Dissociation constants provided by this optimization procedure were assessed by numerical integration. Each individual binding step is represented by a differential equation of the form:

$$\frac{d[AB]}{dt} = [A] \times [B] \times ON\_RATE - [AB] \times k_{off}$$

where A and B represent the two species to the left of an equation in Table 3, and AB is the corresponding binary complex. k_{off} is the rate of dissociation of the AB complex (in units of sec^{-1}) and ON_RATE is the rate of association, which we have taken as 1×10^6 $M^{-1}s^{-1}$ for all binding interactions–a typical diffusion limited value for protein interactions (Northrup and Erickson, 1992). The method of integration was, in most cases, a modified Euler integration with adaptive step size developed specifically for this problem (Bray and Lay, 1994b). This was chosen because it required a smaller number of integrations to achieve a solution than conventional methods such as forth-order Runge Kutta or variable step Runge Kutta algorithms (Press *et al.*, 1992). Each integration provided an estimate of the final, steady state concentration of the state of the system. The concentration of the complex TTWWAA (and in some cases TTWAA) was then compared with target concentrations deduced from the swimming behavior of the bacterium.

Prediction of Swimming Behavior

The relationship between the swimming behavior of the bacterium and the intracellular concentration of TTWWAA depends on the rate of transfer of phosphate groups from the TTWWAA complex to Y and on the influence of Yp on flagellar rotation. An existing model of signaling reactions in bacterial chemotaxis (Bray *et al.*, 1993) provided the basis for evaluating swimming performance for any specified genotype or stimulus condition. Behavior is normally quantitated as the rotational bias, which is the fraction of time the flagella spend in counterclockwise rotation. The current version of the program differs from the original in several ways:

1) The binding interactions between TT, W, and AA are modeled as described in this paper.
2) Autophosphorylation of AA was permitted in all complexes containing AA rather than just in free AA alone.
3) Several rate constants were changed due to recent experimental evidence (Table 1).
4) Autophosphorylation of Y by acetyl phosphate is included (Lukat *et al.*, 1992).
5) The bias of the flagellar switch is calculated simply from the concentration of Yp and a Hill coefficient of 5.5 (Kuo and Koshland, 1989) rather than a complicated model of switch binding.

The active complex of TT, W, and AA (TTWWAA) exhibits a rate of autophosphorylation of AA some 680-fold greater than that of free AA (Stewart, personal communication). The rate of phosphorylation of AA in complexes containing W is the same as that of free AA under conditions of saturating ATP concentration (McNally and Matsumura, 1991). The question of whether the intermediate complex TTWAA forms in appreciable amounts and whether its activity resembles that of AA or of TTWWAA has not been addressed experimentally and was examined in this study.

Intracellular Yp and TTWWAA Concentrations

A crucial link between the concentration of TTWWAA and the swimming behavior of the bacterium is provided by the intracellular concentration of Yp. This protein interacts with the switch complex of the flagellar motor and, if present in sufficiently high quan-

Table 1. Rates of phosphorylation reactions used in the simulation

Reaction	Rate constant	Reference
Autophosphorylation of CheA by ATP[a,b] AA → AAp, WAA → WAAp, WWAA → WWAAp, TTWAA → TTWAAp TTAA → TTAAp	$2.5 \times 10^{-2}\ s^{-1}$	Tawa and Stewart, 1944
Receptor-stimulated autophosphorylation of CheA by ATP[a] TTWWAA → TTWWAAp	$1.7 \times 10^{1}\ s^{-1}$	Stewart, personal communication
Phosphotransfer from CheAp to CheY[c] AAp + Y → AA + Yp, WAAp + Y → WAA + Yp, WWAAp + Y → WWAA + Yp, TTWAAp + Y → TTWAA + Yp, TTWWAAp + Y → TTWWAA + Yp, TTAAp + Y → TTAA + Yp	$3 \times 10^{7}\ M^{-1}\ s^{-1}$	Stewart, personal communication
Autophosphorylation of CheY by acetyl phosphate[a] Y → Yp	$8.8 \times 10^{-2}\ s^{-1}$	Lukat *et al.*, 1992
Autodephosphorylation of CheYp Yp → Y	$3.7 \times 10^{-2}\ s^{-1}$	Lukat *et al.*, 1991
CheZ-stimulated dephosphorylation of CheYp Yp + Z → Y + Z	$5 \times 10^{5}\ M^{-1}\ s^{-1}$	Lukat *et al.*, 1991
Phosphotransfer from CheAp to CheB[c] AAp + B → AA + Bp WAAp + B → WAA + Bp, WWAAp + B → WWAA + Bp, TTWAAp + B → TTWAA + Bp, TTWWAAp + B → TTWWAA + Bp, TTAAp + B → TTAA + Bp	$6 \times 10^{6}\ M^{-1}\ s^{-1}$	Stewart, personal communication
Autodephosphorylation of CheBp[d] Bp → B	$3.5 \times 10^{-1}\ s^{-1}$	Stewart, 1993

[a] The simulation represents autophosphorylation reactions as pseudo-first order reactions with a correction of the form [phosphodonor]/(K_m + [phosphodonor]) applied to these rate constants (the concentrations of ATP and acetyl phosphate are unlikely to change in the few seconds it takes for the swimming response to reach a stable state). Parameters used were [ATP] = 3×10^{-3} M (Bochner and Ames, 1982), $K_{m,ATP} = 3 \times 10^{-4}$ M (Wylie *et al.*, 1988; McNally and Matsumura, 1991; Tawa and Stewart, 1994), [acetyl phosphate] = 10^{-5} M (Pruss and Wolfe, 1994), and $K_{m,acetyl\ phosphate} = 7 \times 10^{-4}$ M (Lukat *et al.*, 1992).

[b] AA autophosphorylation rates have been well characterized for free AA and for the TTWWAA ternary complex. The rates for autophosphorylation of complexes containing TT and/or W in addition to AA are assumed to be the same as for free AA. WWAA autophosphorylation is known to exhibit the same V_{max} as AA (McNally and Matsumura, 1991). Our simulation does not include the fact that WWAA has a much lower K_m for ATP than AA (McNally and Matsumura, 1991); however, this simplification has little consequence at physiological ATP concentration, which is essentially saturating for both reactions. The possibility that communication between TT and AA in the absence of W may result in reduced autophosphorylation (Ames and Parkinson, 1994) for TTAA is not included in our simulation. In a few simulations, the autophosphorylation rate of TTWAA was assumed to be like that of TTWWAA, as noted in the text.

[c] Rates have been measured experimentally only for phosphotransfer from free AAp to Y or B. The rates for phosphotransfer from complexes containing TT and/or W in addition to AAp are assumed to be the same.

[d] The rate constant for autodephosphorylation of Bp is $7 \times 10^{-1}\ s^{-1}$ at 35°C (Stewart, 1993). The simulation used half this value (Stewart, personal communication), to be consistent with the other rate constants, which were measured at 20–25°C.

tities, causes the default counterclockwise rotation of the motor to change to a clockwise rotation (Barak and Eisenbach, 1992; Welch *et al.*, 1993, 1994). The concentration of Yp in the cytoplasm of a wild-type unstimulated bacterium is consequently an important reference point for any calculation of rates of phosphorylation and dephosphorylation. Because there are at present no direct experimental measurements of this concentration, we estimated this value using our computer model. The basis for the calculation was that a mutant lacking TT, W, and Z ($T^-W^-Z^-$) has a rotational bias close to wild type (Liu and Parkinson, 1989). We therefore determined the concentration of Yp generated by the network of phosphorylation and dephosphorylation reactions involving only AA, B, and Y, using experimentally determined values of protein concentrations (see Bray *et al.*, 1993) and rate constants (Table 1). There is more Y than B in the cell (DeFranco and Koshland, 1981; Stock *et al.*, 1985; Kuo and Koshland, 1987; Stock *et al.*, 1991) and phosphotransfer from AAp to Y is faster than to B (Table 1). Thus, the presence or absence of B makes only an ~5% difference in the concentration of Yp in this simulation (our unpublished data), and B can removed from this reaction network, leaving only AA and Y. In this case, a simple kinetic equation can then be written for the steady state formation and breakdown of Yp and solved algebraically, without using the computer simulation (Figure 2). This leads to a quadratic equation for Yp with only one reasonable solution, close to 1.6 μM.

Given that a cell has wild-type bias at this calculated concentration of Yp, and a known Hill coefficient governs interactions between Yp and the switch, it is also possible to derive a simple equation relating bias to Yp, namely:

$$Bias = 1 - \frac{(Yp^{Hill})}{2.333(SetYp^{Hill}) + Yp^{Hill}}$$

where the exponent Hill is the Hill coefficient and SetYp is the Yp concentration in an unstimulated wild-type cell. Note that when there is no Yp, the simulated bias is 1 (i.e., CCW rotation); as Yp increases, the simulated bias approaches 0 (i.e., CW rotation), and when Yp = SetYp, the simulated bias is 0.7 (i.e., wild-type value); all as expected.

The value of Yp can also be used to predict the steady state concentration of the active complex TTWWAA in an unstimulated wild-type bacterium. In such a bacterium, the increased rate of formation of Yp due to the activity of the complex must be balanced by the increased loss of Yp due to Z activity. Current estimates of the rates of these two reactions lead to a concentration of TTWWAA close to 1 μM. Precise target values used for wild-type and mutant strains were obtained by a process of titration using the chemotactic simulation (Table 2). The above equation can be used to determine the Yp concentration that corresponds to a given bias; one can then work backward to deduce the TTWWAA concentration that yields the desired value of Yp.

Network Evaluation

To summarize at this point: each individual network (that is, each set of binding equilibria and their dissociation constants) was evaluated by calculating the concentration of the complex TTWWAA (or in some cases TTWAA plus TTWWAA) the network would produce given specific starting levels of TT, W, and AA. This was done for each of the mutant genotypes in the test set (Table 2). The steady state concentrations of the complexes reached were then compared with the target values predicted from the steady state, unstimulated, swimming behavior for each mutant. Absolute differences between the simulated and target TTWWAA concentrations for each of the mutant types were added together and the sum was used as a cost value. Cost values were consequently smaller the more closely the performance of the simulation matched test criteria, and a cost less than 10^{-7} M ensured that the bacterial strains had the desired swimming behavior.

RESULTS

10-Reaction Network

There are a number of experimental observations concerning the binding interactions between TT, W and AA as follows:

1) Both TT and AA normally exist in solution as dimeric species whereas W is monomeric (Milligan and Koshland, 1988; Gegner and Dahlquist, 1991).
2) W and AA form a complex WWAA (Gegner and Dahlquist, 1991; McNally and Matsumura, 1991).
3) W binds to TT (Gegner *et al.*, 1992).
4) A ternary complex forms between TT, W, and AA and has a probable composition of TTWWAA (Gegner *et al.*, 1992).
5) Ternary complex formation is not affected by ligand binding, phosphorylation, or the phosphotransfer substrates Y or B (Gegner *et al.*, 1992).
6) Binding of AA to TT depends on W, which forms a link between the two (Gegner *et al.*, 1992) and therefore opens the possibility of the complex TTWAA.

These observations can be used to formulate pathways for formation of the TTWWAA complex. There are 10 theoretically possible binding reactions between TT, W, and AA given the following constraints: 1) TT and AA maintain their dimeric state, 2) TT and AA interact only through W, and 3) no complex contains more than one TT, one AA, or two W molecules (Table 3, reactions #1–10).

The network derived from binding steps 1–10 in Table 3 has a set of 10 coupled binding constants each of which can take a range of values. The number of independent variables is less than this, however, because of thermodynamic constraints. The difference in free energy between any two states of the system is fixed. Therefore, the free energy changes in a series of binding equilibria that connect these two states must always add to this value whatever the individual steps between the states. For this reason, there are only six independent variables in this network, and the other four K_d values can be deduced (Figure 3).

Multiple attempts were made to optimize the network on the basis of the set of test criteria shown in Table 2. A range of starting K_d values was used,

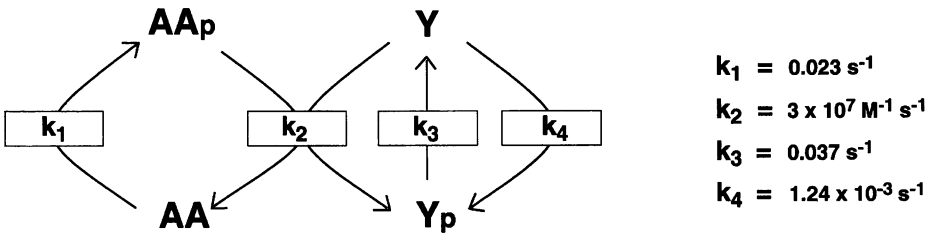

Figure 2. Phosphotransfer reactions used to estimate the steady state concentration of Yp. The reactions affecting Yp in the mutant strain $T^-W^-Z^-$, which has approximately wild-type swimming bias, are shown except for formation and destruction of Bp. Reactions shown are as follows: 1) autophosphorylation of AA to AAp, 2) phosphotransfer of phosphate from AAp to Y, 3) autodephosphorylation of Yp to produce Y, and 4) phosphorylation of Y by transfer from acetyl phosphate. Reaction rates k_1-k_4 are derived from Table 1 and take into account phosphodonor concentration. The total concentration of AA-containing species was taken to be 2.5 μM and that of Y-containing species was taken to be 10 μM (see Bray *et al.*, 1993). Algebraic solution of equations derived from the above reactions gives a steady state concentration of Yp of 1.63 μM.

Table 2. Criteria used for network optimization

Experimental observations			Simulation targets	
Genotype[a]	Rotation[b]	References	Bias	[TTWWAA] (M)[c]
Wildtype	Wildtype	Block *et al.*, 1982	0.70	1.13×10^{-6}
10 T	CCW	Liu and Parkinson, 1989	>0.95	$<8 \times 10^{-8}$
10 W	CCW	Liu and Parkinson, 1989; Sanders *et al.*, 1989	>0.95	$<8 \times 10^{-8}$
10 T, 10 W	Wildtype	Liu and Parkinson, 1989	0.70	1.13×10^{-6}
10 A	Wildtype/ CCW	Parkinson, personal communication; Bourret, unpublished results	~0.8	1.02×10^{-6}
10 A, 10 W	CCW	Liu and Parkinson, 1989; Bray *et al.*, 1993	>0.95	$<8 \times 10^{-8}$

[a] A genotype of "10 W" indicates a strain in which CheW is expressed at 10 times the normal level, with other genes being expressed at the wild-type level. Note that the extent of overproduction was not measured experimentally; it is assumed to be 10-fold for the purposes of simulation.

[b] Direction of flagellar rotation in strains overproducing the indicated proteins. "Wildtype" indicates the mix of CCW and CW rotation characteristic of a wild-type cell.

[c] The concentration of the active complex needed to produce the desired bias was estimated by a form of titration in which the swimming behavior of a range of networks with different TTWWAA concentrations was evaluated by the chemotactic simulation.

with individual K_d values ranging systematically, in powers of 10, between 10^{-5} M and 10^{-8} M, thereby encompassing the usual range of dissociation constants for protein associations in cells. Individual tests typically involved a total of 3,000 selection steps, each of which entailed a numerical integration that might take 10^6 steps or more. Because individual tests might take several hours of CPU time on a Macintosh Quadra 950 or a Sun SPARC workstation, the systematic evaluation of some networks took a week or more to complete. Eventually, sets of K_d values that gave cost values less than 10^{-8} M were obtained; one such set is given in Table 3. When these K_d values were installed in the full simulation, they produced phenotypes that corresponded to the experimentally determined test values.

The K_d values obtained in successive runs and from different starting points showed significant variation, reflecting the random nature of the selection process and the fact that a finite cost value was used as a target. When solutions with cost values less than 10^{-8} M were compared, however, individual K_d values were seen to be clustered around typical values: average values obtained for the 10-

Table 3. Examples of sets of K_d values derived by optimization to meet the target criteria of Table 2

		K_d (M)			
	Binding step[a]	Seven-reaction network	10-Reaction network	12-Reaction network	12*-Reaction network[b]
1	TT + W ↔ TTW	1.57×10^{-9}	5.18×10^{-10}	3.65×10^{-9}	4.17×10^{-8}
2	TTW + W ↔ TTWW	4.79×10^{-8}	2.23×10^{-8}	5.11×10^{-8}	1.95×10^{-7}
3	W + AA ↔ WAA	4.28×10^{-9}	2.16×10^{-9}	8.94×10^{-9}	6.22×10^{-8}
4	WAA + W ↔ WWAA	1.23×10^{-7}	7.25×10^{-8}	1.02×10^{-7}	1.06×10^{-6}
5	TT + WAA ↔ TTWAA	—	7.16×10^{-6}	2.97×10^{-4}	5.21×10^{-8}
6	TTW + AA ↔ TTWAA		2.99×10^{-5}	7.27×10^{-4}	7.77×10^{-8}
7	TTWAA + W ↔ TTWWAA	—	6.10×10^{-11}	7.87×10^{-12}	3.44×10^{-6}
8	TTW + WAA ↔ TTWWAA	8.36×10^{-7}	8.43×10^{-7}	6.40×10^{-7}	4.30×10^{-6}
9	TTWW + AA ↔ TTWWAA	7.47×10^{-8}	8.16×10^{-8}	1.12×10^{-7}	1.37×10^{-6}
10	TT + WWAA ↔ TTWWAA	1.07×10^{-8}	6.02×10^{-9}	2.29×10^{-8}	1.69×10^{-7}
11	TT + AA ↔ TTAA	—	—	3.93×10^{-5}	1.74×10^{-7}
12	TTAA + W ↔ TTWAA	—	—	6.76×10^{-8}	1.86×10^{-8}

[a] Candidate binding steps used in the optimization routine. TT, W, and AA are the starting components. TTWWAA is the active complex. Various networks were built using binding steps drawn from this list and tested by the optimization procedure.

[b] TTWAA is endowed with activity equivalent to TTWWAA in the 12*-reaction network.

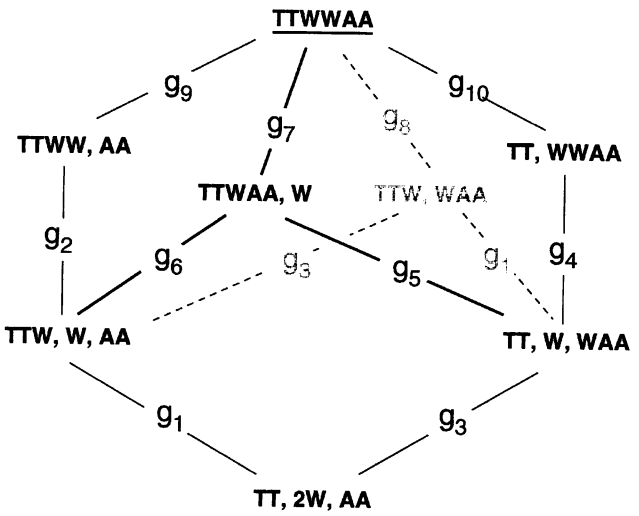

Figure. 3. The network of 10 binding steps from Table 3 shown together with their free energy changes. Each state of the system comprises a set of protein species, such as TTW plus WAA (TTW, WAA), which can be converted to one or more other states by reversible binding. The starting state is (TT, 2W, AA) and the active complex is TTWWAA. Ten different binding equilibria exist connecting these various states, each of which has an associated change in standard Gibbs energy **g**. Because the difference in free energy of any two states is fixed (albeit unknown), whatever the pathway of binding steps from one to the other, their individual free energy changes (**g** values) must add up to the same value. This constraint means that the free energy changes of some steps can be deduced from those of other steps, as follows: $\mathbf{g}_2 = \mathbf{g}_3 + \mathbf{g}_8 - \mathbf{g}_9$; $\mathbf{g}_4 = \mathbf{g}_1 + \mathbf{g}_8 - \mathbf{g}_{10}$; $\mathbf{g}_6 = \mathbf{g}_3 + \mathbf{g}_5 - \mathbf{g}_1$; $\mathbf{g}_7 = \mathbf{g}_1 + \mathbf{g}_8 - \mathbf{g}_5$. Because the free energy change of a reaction is related to its dissociation constant (K_d) by $\mathbf{g} = RT\ln K_d$, the above expression for $\mathbf{g}_2$ is equivalent to the following:

$$K_d(2) = \frac{K_d(3) \times K_d(8)}{K_d(9)}$$

and similar relationships can be written for $K_d(4)$, $K_d(6)$, and $K_d(7)$.

reaction network, together with the standard error of the mean, are given in Table 4.

7-Reaction Network

Among the various solutions that the optimization routine produced for the 10-reaction network, the K_d values for the binding steps involved in the formation and destruction of TTWAA frequently took on extreme values compared with the K_d values for other binding steps. The two binding steps leading to TTWAA (TTW + AA = TTWAA and TT + WAA = TTWAA) both had relatively large K_d values compared with other steps whereas step #7 (TTWAA + W = TTWWAA) in which TTWAA is converted to the active complex had a K_d lower than any other (Table 4). The consequence of these K_d values was that the concentration of TTWAA at equilibrium was usually very small. We therefore deleted these reactions from the network and attempted to obtain solutions to the test criteria in a new network composed of seven reactions and lacking TTWAA entirely. This effort was successful (a sample solution is given in Table 3), indicating that it is not necessary to form TTWAA to meet the target criteria.

No systematic attempt has been made to determine the smallest possible network that permits a solution to the constraints listed in Table 2. However, solutions were found to a network with six reactions derived from the 7-reaction network by deleting reaction #8 (our unpublished data).

12-Reaction Network

Although direct binding of TT and AA has not been observed (Gegner *et al.*, 1992) there is genetic and biochemical evidence that TT can regulate AA activity in the absence of W (Liu and Parkinson, 1989; Ames and Parkinson, 1994). A network permitting formation of TTAA was therefore constructed by adding reactions #11 and 12 (Table 3) to the 10-reaction network. Because of thermodynamic constraints, 5 of the 12 K_d values could be derived from the others, leaving seven independent variables to be optimized. Multiple solutions were obtained by optimization, one of which is given in Table 3.

High TTWAA Activity

The carboxy terminal domain of AA is necessary for regulation of CheA kinase activity by TT and W (Bourret *et al.*, 1993). An AA heterodimer in which one subunit is missing the C-terminal regulatory domain should form at most one functional connection to TT. The properties of such heterodimers in the presence of TT and W have been extensively investigated, but it remains unclear whether TT can regulate AA under these circumstances (Swanson *et al.*, 1993a; Wolfe *et al.*, 1994).

The analogous species in our simulation is TTWAA, which has not been observed experimentally. To see whether computer simulation could shed some light on this debate, the effect of assigning the same high level of CheA phosphorylation to TTWAA as TTWWAA was explored for the 10- and 12-reaction networks. The optimization routine was asked to find K_d values that would generate the Table 2 target values for [TTWWAA] with [TTWAA + TTWWAA] instead. Solutions were obtained for the 12*-reaction (see Table 3), the lowest cost value achieved being 4.7×10^{-8} M. No solution was found for the 10-reaction case.

Simulation of TT, W, or AA Overproduction

The simulation was used to predict flagellar rotational bias as a function of TT, W, or AA concentration for each of the four networks described in

Table 4. Average K_d values obtained in solutions to the 7-reaction and 10-reaction networks

	Binding step	K_d (M) 7-reaction	K_d (M) 10-reaction
1	T + W ↔ TTW	$1.00 \pm 0.16 \times 10^{-9}$	$8.06 \pm 0.93 \times 10^{-10}$
2	TTW + W ↔ TTWW	$6.68 \pm 0.80 \times 10^{-8}$	$5.42 \pm 0.63 \times 10^{-8}$
3	W + AA ↔ WAA	$2.96 \pm 0.24 \times 10^{-9}$	$3.40 \pm 0.30 \times 10^{-9}$
4	WAA + W ↔ WWAA	$1.88 \pm 0.21 \times 10^{-7}$	$1.63 \pm 0.21 \times 10^{-7}$
5	TT + WAA ↔ TTWAA	—	$2.62 \pm 0.08 \times 10^{-6}$
6	TTW + AA ↔ TTWAA	—	$1.06 \pm 0.64 \times 10^{-3}$
7	TTWAA + W ↔ TTWWAA	—	$1.03 \pm 0.17 \times 10^{-10}$
8	TTW + WAA ↔ TTWWAA	$9.33 \pm 0.32 \times 10^{-7}$	$8.73 \pm 0.33 \times 10^{-7}$
9	TTWW + AA ↔ TTWWAA	$6.58 \pm 0.51 \times 10^{-8}$	$7.71 \pm 0.51 \times 10^{-8}$
10	TT + WWAA ↔ TTWWAA	$1.04 \pm 0.15 \times 10^{-8}$	$9.95 \pm 1.26 \times 10^{-9}$

Optimizations were performed repeatedly on these networks using different sets of starting K_d values. Values obtained for the binding reactions are shown together with the standard error of the mean. Note that because K_d values for each binding step were averaged independently, the values given in this table–in contrast to those given in Table 3–do not in themselves constitute a solution to the optimization. That is, a network of reactions possessing the above K_d values will not give the correct chemotactic behavior, nor will it conform to the thermodynamic constraints discussed in Figure 3.

Table 3 (Figure 4). The optimization routine ensures that all networks generate the target bias of ~0.7 at wild-type protein concentration and the appropriate bias (~1 for TT or W and ~0.8 for AA) at 10 × wild-type protein concentration. The predicted bias at other protein concentrations reveals several interesting features.

First, the absence of TT, W, or AA is predicted to result in a bias of 1, consistent with experimental observation (Parkinson, 1978; Liu and Parkinson, 1989). Second, bias is much more sensitive to TT, W, or AA concentration and reaches much lower values in the case where TTWAA has high activity (12*-reaction network) than when it does not (7-, 10-, and 12-reaction networks). This may be an experimentally testable prediction. The three networks with low TTWAA activity make essentially indistinguishable predictions. Third, all networks predict that bias differs from 1 only over a very narrow range of W concentrations. Finally, one might expect that increasing the concentration of the AA kinase would in turn lead to an increase in Yp concentration and hence a decrease in bias. Instead, all networks make the counterintuitive prediction that increasing AA leads to a bias of 1, which implies that Yp actually *decreases* when AA increases.

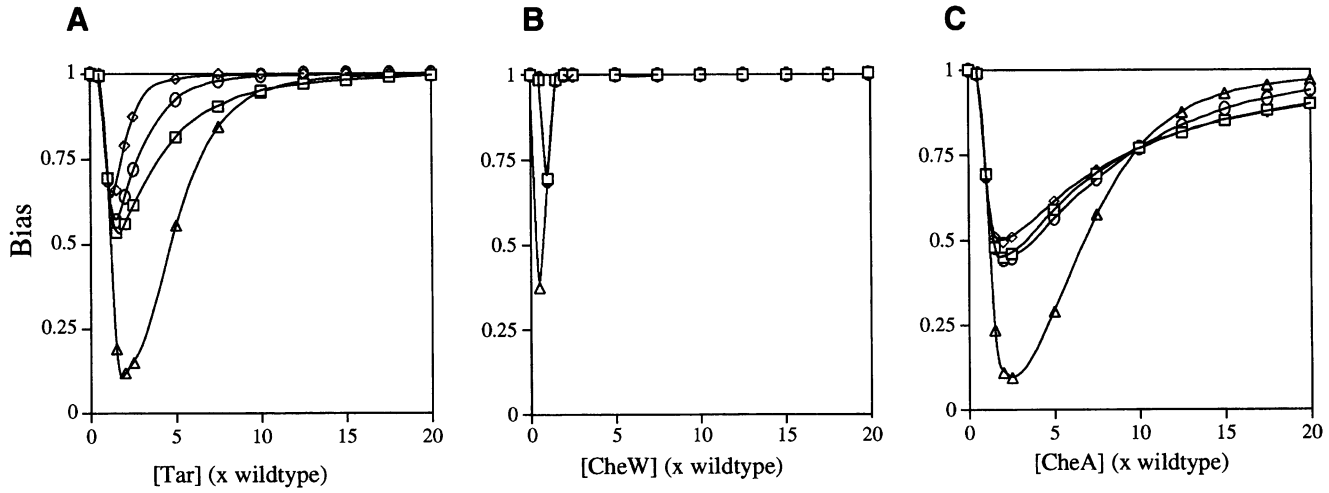

Figure 4. Predicted effect of overexpression of TT, W, or AA on rotational bias for each of the four networks whose K_d values are given in Table 3: 7-reaction, □; 10-reaction, ◇; 12-reaction, ○; 12*-reaction, △. The circle, diamond, and square plots in the W panel superimpose.

The solutions listed in Table 3 were also used to predict the concentrations of the various proteins and oligomeric species involved in formation of the receptor complex. This analysis revealed a number of general features of the solutions (illustrated in Figure 5 for the case of the 12-member binding network). In a wild-type organism, the most abundant protein species was the active complex TTWWAA. Expression of TT in elevated amounts led to a reduction of this active complex and formation of TT-containing species–chiefly TT itself and TTW. Evidently, therefore, the smooth phenotype observed in this mutant may be explained by the sequestration of W into an inactive complex (TTW) thereby reducing the amount available to form TTWWAA. Similarly, in mutants in which W is overexpressed, the large amounts of TTWW and WWAA produced serve to reduce the amounts of TT and AA available for active complex formation. Co-overexpression of both TT and W results primarily in formation of complexes containing both proteins (TTW and TTWW) and restores essentially wild-type levels of the active complex.

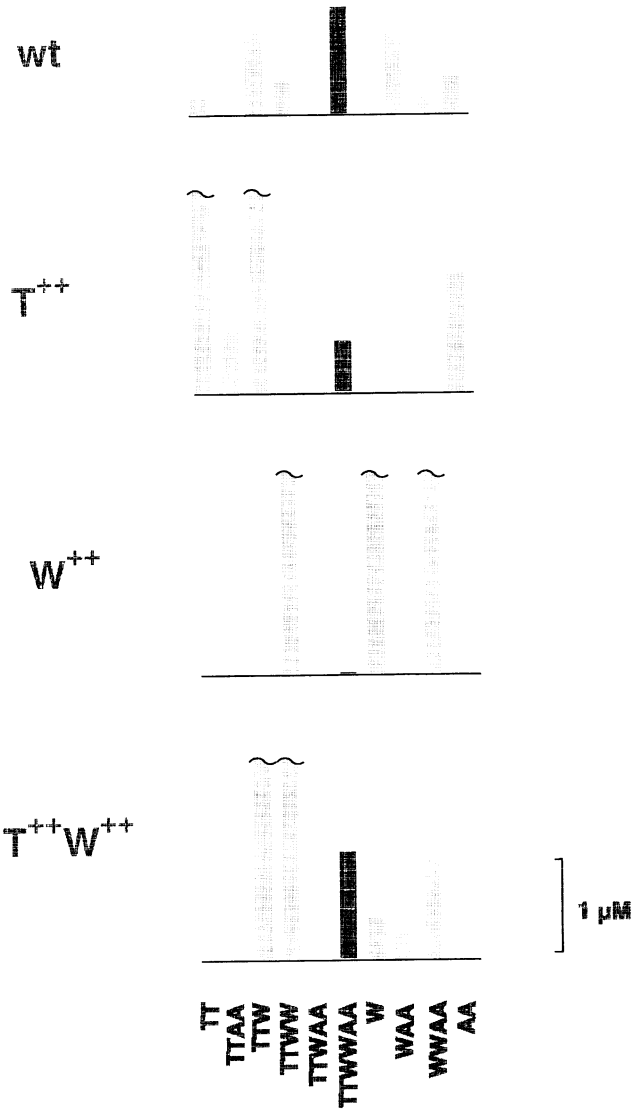

Figure 5. Concentrations of oligomers containing TT, W, and AA expected for different genotypes. The K_d values listed in Table 3 for the 12-reaction network were used to predict the steady state concentrations of TT, W, and AA and of the oligomeric complexes formed from these proteins. Overexpression of TT and/or W was at 10 times wild-type concentration. Concentrations are shown as vertical bars. The active complex (TTWWAA) is shown in black, the others in gray. Truncated bars, topped with ~, indicate a concentration greater than 2 μM.

Dissociation Constants

The dissociation constants of two individual steps have been measured experimentally with purified proteins: a dissociation constant of 17 μM was obtained for the reaction W + AA ↔ WAA (Gegner and Dahlquist, 1991), and a dissociation constant of ~10 μM was obtained for TT + W ↔ TTW (Gegner *et al.*, 1992). It was therefore important to examine the dissociation constants predicted for these particular binding steps by computer simulation. All of the networks examined give dissociation constants three to four orders of magnitude smaller than the experimental values (Table 5). Attempts to "clamp" the two binding steps to the experimental values during the simulation were unsuccessful and failed to produce solutions: the largest dissociation constants achieved for these two reactions were 4.2×10^{-8} M and 6.2×10^{-8} M, respectively, obtained with the 12*-network.

The concentrations of TT, W, or AA in the mutant bacteria used to define the boundary conditions for the optimization routine have not been measured experimentally and were arbitrarily set at 10 times the wild-type concentration (Table 2). We also ran a series of optimizations in which proteins were assumed to be overexpressed 30-fold instead of 10-fold, and found that this reduced the discrepancy between experimental and simulated K_d values by a factor of ~10. The largest K_d values obtained in this series were 5.2×10^{-7} M for the binding of TT and W and 7.8×10^{-7} M for the binding of W and AA (our unpublished data). The basis on which we selected values of intracellular protein concentrations, and one possible explanation for the very striking discrepancy between simulated and experimental K_d values, are provided in the DISCUSSION section.

DISCUSSION

Multiprotein Complex Formation

Many proteins in living cells exist as part of multimeric aggregates, such as enzyme complexes, prote-

Table 5. Comparison of experimental and simulated K_d values for W binding to TT or AA

		Kd (M)			
			Maximum simulated value[b]		
	Binding step	Experimental value[a]	7-reaction network	10-reaction network	12*-reaction network
#1	TT + W ↔ TTW	$\sim 1 \times 10^{-5}$	3.12×10^{-9}	7.00×10^{-9}	4.20×10^{-8}
#3	W + AA ↔ WAA	1.7×10^{-5}	2.78×10^{-9}	9.65×10^{-9}	6.21×10^{-8}

[a] References are Gegner *et al.* (1992) for reaction #1 and Gegner and Dahlquist (1991) for reaction #3.

[b] The different networks are composed of the binding steps listed in Table 3. The largest K_d values generated in multiple solutions for each network are given in this table.

asomes, and centrioles. More specifically, multiprotein complexes are also a common feature of eukaryotic signal transduction pathways, including those mediated by binding domains such as SH2 and SH3, (Cohen *et al.*, 1995; Pawson, 1995), G proteins (Clapham and Neer, 1993; Conklin and Bourne, 1993), the MAP kinase cascade (Choi *et al.*, 1994; Marcus *et al.*, 1994), the retinoblastoma protein (Welch and Wang, 1995), or compartmentalized serine/threonine kinases (Mochly-Rosen, 1995). The aggregates form by the diffusion-limited association of their component proteins and thus their concentration in the cell–and hence the level of their biological activity–is in general thought to be controlled by the law of mass action. In this case, if the number of component proteins present and the affinity with which they bind to each other were known, then it might be possible to calculate the concentration of the active multiprotein complex. In reality, however, for anything other than complexes with very few components, the equilibrium state is given by a set of nonlinear simultaneous equations that cannot be solved analytically. Furthermore, even if all of the dissociation constants had been measured under defined conditions, which is almost never the case, then there is still the problem of estimating their true value in the crowded conditions of the interior of a living cell.

In the present study we have attempted to use optimization techniques to learn how one set of proteins associates in the living cell. Bacterial chemotaxis is arguably the best understood system of intracellular signaling and is the particular case explored here. Many mutant bacteria have been isolated in which one or more of the proteins of the TTWWAA complex have been deleted or overexpressed and the consequences for chemotactic behavior have been measured experimentally. This provides a set of boundary conditions for our optimization scheme, and values for binding constants that reproduce the mutant phenotypes can then be estimated. This approach could in the future be applicable to other signal pathways. For example, overexpression of the CD4 receptor reduces activation of the $p56^{lck}$ tyrosine kinase in thymocytes, apparently by disrupting complex formation (Nakayama *et al.*, 1993). Similarly, overexpression of a fragment of the retinoblastoma protein results in inhibition of activity of the full length protein, again apparently by disrupting complex formation (Welch and Wang, 1995).

Simulated Overexpression of Chemotaxis Proteins

Overexpression of the TT, W, or AA proteins leads to phenotypes that are unexpected and could not have been easily predicted. Overexpression of TT gives the same smooth phenotype as deletion of TT (Liu and Parkinson, 1989); overexpression or deletion of W gives the same, smooth swimming, phenotype (Parkinson, 1978; Liu and Parkinson, 1989; Sanders *et al.*, 1989); overexpression of TT and W together, in contrast to their individual overexpression, restores the wild-type swimming pattern (Liu and Parkinson, 1989). Overproduction of AA is less well characterized, but the results of our unpublished studies show that it gives a slightly higher bias than wild type bias. The optimization scheme leads to a computer simulation that faithfully reproduces each of these behaviors by changing the distribution of TT, W, and AA among the various possible complexes (and hence the amount of the active TTWWAA species) under different circumstances. The AA overproduction phenotype is particularly noteworthy. One might intuitively expect that increasing amounts of the CheA kinase would lead to more Yp and hence a reduced bias; in fact this is exactly what a previous, simpler version of the simulation predicted (Bray *et al.*, 1993). In contrast, the current simulation correctly predicts that increasing AA increases the bias (Figure 4), a result which stems from the large difference in autophosphorylation activity between TTWWAA and other complexes containing AA.

In all simulated networks, overexpression of W had a more potent effect in increasing bias than did in overproduction of TT (Figure 4). There is some evidence that this is reproduced in vivo, because overexpression of W in a Z^- background gives a CCW phenotype whereas overexpression of receptor in the same background results in wild-type swimming behavior (Liu and Parkinson, 1989). The solutions obtained were also consistent with other experimental evidence, including the phenotypes of 23 other mutants that have been studied experimentally and that were listed in a previous publication (Bray *et al.*, 1993).

Potential Role of TTWAA

There is experimental evidence that a complex containing only one link between TT and AA may be fully functional; however, related experimental results cannot be easily explained by this model (Wolfe *et al.*, 1994). The alternate approach of computer simulation has provided some information about the putative TTWAA complex. The existence of such a complex is not necessary to account for the mutant phenotypes listed in Table 2 (e.g. see 7-reaction network of Table 3). The TTWAA complex could nevertheless exist: it might, for example, be needed to fulfill requirements not demanded in this version of the simulation. Alternatively, TTWAA might be formed gratuitously, as a necessary by-product of the binding steps that lead to TTWWAA.

The computer simulation indicates that if TTWAA does exist and has the high autophosphorylation activity characteristic of TTWWAA, then binding steps in addition to those of the 10-reaction network (see Table 3) are necessary to account for the mutant phenotypes of Table 2. This is because overexpression of TT leads to loss of TTWWAA activity (Liu and Parkinson, 1989). In the 10-reaction network, excess TT pulls W out of other complexes to form TTW. This reduces TTWWAA concentration but leads to an increase in free AA and hence TTWAA. If TTWWAA and TTWAA are of comparable activity, then the excess TT phenotype cannot result. A likely solution based on available experimental evidence (Liu and Parkinson, 1989; Ames and Parkinson, 1994) is to postulate direct binding between TT and AA in spite of the failure to observe such binding in vitro (Gegner *et al.*, 1992). In the 12-reaction network, excess TT also leads to high levels of TTW, but now some of the AA freed from complexes with W can be sequestered in a nonproductive TTAA complex, unavailable for TTWAA formation (Figure 5).

Finally, a network in which TTWAA has high autophosphorylation activity is predicted to generate very different behavior than networks with low TTWAA activity when TT, W, or AA concentrations are changed (Figure 4). Computer simulation thus suggests an experimental approach that could indicate whether TTWAA has high or low activity, i.e., a careful examination of bias as a function of TT, W, or AA expression. In fact, Sanders *et al.* (1989) have reported that "at no level of CheW expression tested did the cells tumble more frequently than wild-type cells." This result appears to be consistent with low but not high TTWAA activity in our simulations (Figure 4). Specifically, the 10- and 12-reaction networks predict that the minimum bias occurs at wild-type W concentration, and only the 12*-network has a bias < 0.7 at any W concentration.

Binding Constants

An important discrepancy between theory and experiment emerged in this study. For all of the networks examined, the predicted dissociation constants for two reactions, TT + W $\leftrightarrow$ TTW and W + AA $\leftrightarrow$ WAA, were much smaller than the experimentally measured values, indicating a much tighter binding. This discrepancy could arise from a variety of sources. The rates of phosphorylation and dephosphorylation reactions or the binding constants for protein/protein interactions could be very different in the cell than measured in vitro due to protein modifications or association with other factors presently not identified. Another possibility is that the effective concentration of the species W or AA in the vicinity of TT might be much higher than predicted simply by dividing the number of molecules by the volume of the cell. A more accurate simulation would have to include any restriction of particular proteins to subcompartments within the cytoplasm. The higher the concentration of TT, W, and AA in the cytoplasm, the weaker the binding would need to be to produce a specific concentration of TTWWAA complex. Note that when we increased the dosage of overexpression mutants (thereby increasing the concentration of TT, W, and AA in these mutants) then the K_d values we obtained were larger.

A major contribution to the discrepancy between experimental and simulated K_d values is likely to be made by macromolecular crowding. The cytoplasm of living cells is a highly concentrated aqueous solution of large and small molecules and *E. coli* has been estimated to contain collectively about 340 g/liter of total RNA and protein (Zimmerman and Trach, 1991). Steric repulsion between macromolecules at these high concentrations causes profound changes in a variety of biochemical processes, including the association of proteins into macromolecular complexes (Minton, 1981). Thus, a recent review on macromolecular crowding states that "... under conditions of volume occupancy comparable to those found in vivo .... macromolecular associations are predicted to exceed those in solution by as much as several orders of magnitude" (Zimmerman and Minton, 1994). In other

words, if the experimental measurements of binding between CheW, CheA, and Tar had been made under conditions more closely approximating the interior of the cell, then the K_d values obtained would have been closer to those obtained in our simulation.

Additional Network Solutions

The range of solutions obtained for both 10- and 12-reaction networks indicated that the system was overdetermined; that is, there appear to be more variable parameters than are needed to find a solution. Some of the K_d values obtained in the solutions were also consistently very large (a weak binding), suggesting that these particular reactions might be of relatively little importance in the cell. This led us to explore simpler networks with seven binding steps (Table 3) and another set of reactions with only six binding steps has been found. Other solutions may well exist, and it will be interesting to search for the smallest network of binding steps that can meet the behavioral boundary conditions.

It should be noted, however, that a blind insistence on the smallest possible number of binding steps will not necessarily lead to the simplest solution or to one more likely to exist in the living cell. Indeed, Occam's razor could lead to a system of 12 reactions and its associated set of oligomeric intermediates, depending upon how the cut is made, because it is produced by the reiteration of binding steps known to exist. If TT binds to W, then why should an oligomeric complex containing TT not also bind to W, or a complex containing W not bind to TT? Because we do not have direct evidence for the number and types of intermediate oligomeric that exist in the cell, the most important conclusion that can be reached is that some solutions, at least, exist. That is, that sets of binding reactions can be constructed that fulfill the observed phenotypes.

Conclusion

The principal conclusions of this study are as follows:
1) It is possible to find by a process of optimization sets of binding equilibria between TT, W, and AA that fulfill test criteria based on the known phenotypes of specific mutants overexpressing TT, W, or AA.
2) In these computer-based solutions, the smooth swimming of mutants with overexpressed TT or W results from sequestration of other components of the ternary complex into inactive complexes.
3) Formation of the partial complex TTWAA is not essential to fulfill the test criteria. However, if TTWAA is formed, then its level of autophosphorylation activity will influence which types of binding equilibria are possible.
4) The K_d values of binding equilibria predicted by computer-based optimization are all several orders of magnitude smaller (implying tighter binding) than the values of two binding steps that have been measured experimentally. At least part of this discrepancy may be attributed to the high concentration of macromolecules in the cell cytoplasm, which causes major increases in the strength of association between protein molecules.

Optimization methods provide a potentially powerful method to analyze intracellular signaling reactions. As illustrated in the present study, they allow rates of reactions and binding constants in complex networks to be selected on the basis of the final phenotype they confer on the cell. In this way one can endeavor to reconcile experimental evidence obtained from biochemical studies of purified proteins with that obtained from the physiological performance of the entire cell. Evidently, in view of the large discrepancies in binding constants that exist between theory and experiment, we are still a long way from having an accurate picture of the molecular events that carry signals to the flagellar motor. However, our present results do show that a set of physically reasonable binding constants can be found using this approach that are able to fulfill one set of mutant criteria. There seems no reason in principle why the acquisition of further data from in vivo and in vitro sources together with the use of more powerful computers should not provide an increasingly accurate picture of complex networks of intracellular signaling reactions.

ACKNOWLEDGMENTS

We thank Julian Lewis, John Albery, Heinrik Kacser, and Stephen Lay for advice, and Rick Stewart and Alan Wolfe for comments on the manuscript. We also thank Rick Stewart and Sandy Johnson for providing us with their unpublished data. This work was supported by a grant from the Medical Research Council to D.B.

REFERENCES

Ames, P., and Parkinson, J.S. (1994). Constitutively signaling fragments of Tar, the *Escherichia coli* serine chemoreceptor. J. Bacteriol. *176*, 6340–6348.

Barak, R., and Eisenbach, M. (1992). Correlation between phosphorylation of the chemotaxis protein CheY and its activity at the flagellar motor. Biochemistry *31*, 1821–1826.

Block, S.M., Segall, J.E., and Berg, H.C. (1982). Impulse responses in bacterial chemotaxis. Cell *31*, 215–226.

Bochner, B.R., and Ames, B.N. (1982). Complete analysis of cellular nucleotides by two-dimensional thin layer chromatography. J. Biol. Chem. *257*, 9759–9769.

Borkovich, K.A., Alex, L.A., and Simon, M.I. (1992). Attenuation of sensory receptor signaling by covalent modification. Proc. Natl. Acad. Sci. USA *89*, 6756–6760.

Borkovich, K.A., Kaplan, N., Hess, J.F., and Simon, M.I. (1989). Transmembrane signal transduction in bacterial chemotaxis involves ligand-dependent activation of phosphate group transfer. Proc. Natl. Acad. Sci. USA *86*, 1208–1212.

Borkovich, K.A., and Simon, M.I. (1990). The dynamics of protein phosphorylation in bacterial chemotaxis. Cell *63*, 1339–1348.

Bourret, R.B., Borkovich, K.A., and Simon, M.I. (1991). Signal transduction pathways involving protein phosphorylation in prokaryotes. Annu. Rev. Biochem. *60*, 401–441.

Bourret, R.B., Davagnino, J., and Simon, M.I. (1993). The carboxy-terminal portion of the CheA kinase mediates regulation of autophosphorylation by transducer and CheW. J. Bacteriol. *175*, 2097–2101.

Bray, D., Bourret, R.B., and Simon, M.I. (1993). Computer simulation of the phosphorylation cascade controlling bacterial chemotaxis. Mol. Biol. Cell *4*, 469–482.

Bray, D., and Lay, S. (1994a). Computer simulated evolution of a network of cell-signalling molecules. Biophys. J. *66*, 972–977.

Bray, D., and Lay, S. (1994b). Rapid numerical integration algorithm for finding the equilibrium state of a system of coupled binding reactions. Comp. Appl. Biosci. *10*, 471–476.

Choi, K.-Y., Satterberg, B., Lyons, D.M., and Elion, E.A. (1994). Ste5 tethers multiple protein kinases in the MAP kinase cascade required for mating in *S. cerevisiae*. Cell *78*, 499–512.

Clapham, D.E., and Neer, E.J. (1993). New roles for G-protein $\beta\gamma$-dimers in transmembrane signalling. Nature *365*, 403–406.

Cohen, G.B., Ren, R., and Baltimore, D. (1995). Modular binding domains in signal transduction proteins. Cell *80*, 237–248.

Conklin, B.R., and Bourne, H.R. (1993). Structural elements of Gα subunits that interact with G$\beta\gamma$, receptors, and effectors. Cell *73*, 631–641.

DeFranco, A.L., and Koshland, D.E., Jr. (1981). Molecular cloning of chemotaxis genes and overproduction of gene products in the bacterial sensing system. J. Bacteriol. *147*, 390–400.

Gegner, J.A., and Dahlquist, F.W. (1991). Signal transduction in bacteria: CheW forms a reversible complex with the protein kinase CheA. Proc. Natl. Acad. Sci. USA *88*, 750–754.

Gegner, J.A., Graham, D.R., Roth, A.F., and Dahlquist, F.W. (1992). Assembly of an MCP receptor, CheW, and kinase CheA complex in the bacterial chemotaxis signal transduction pathway. Cell *70*, 975–982.

Hazelbauer, G.L., Yaghmai, R., Burrows, G.G., Baumgartner, J.W., Dutton, D.P., and Morgan, D.G. (1990). Transducers: transmembrane receptor proteins involved in bacterial chemotaxis. In: Biology of the Chemotactic Response, ed. J.P. Armitage and J.M. Lackie, Cambridge, UK: Cambridge University Press, 107–134.

Hess, J.F., Bourret, R.B., Oosawa, K., Matsumura, P., and Simon, M.I. (1988a). Protein phosphorylation and bacterial chemotaxis. Cold Spring Harbor Symp. Quant. Biol. *53*, 41–48.

Hess, J.F., Oosawa, K., Kaplan, N., and Simon, M.I. (1988b). Phosphorylation of three proteins in the signaling pathway of bacterial chemotaxis. Cell *53*, 79–87.

Kuo, S.C., and Koshland, D.E., Jr. (1987). Roles of *cheY* and *cheZ* gene products in controlling flagellar rotation in bacterial chemotaxis of *Escherichia coli*. J. Bacteriol. *169*, 1307–1314.

Kuo, S.C., and Koshland, D.E., Jr. (1989). Multiple kinetic states for the flagellar motor switch. J. Bacteriol. *171*, 6279–6287.

Liu, J.D., and Parkinson, J.S. (1989). Role of CheW protein in coupling membrane receptors to the intracellular signaling system of bacterial chemotaxis. Proc. Natl. Acad. Sci. USA *86*, 8703–8707.

Lukat, G.S., Lee, B.H., Mottonen, J.M., Stock, A.M., and Stock, J.B. (1991). Roles of the highly conserved aspartate and lysine residues in the response regulator of bacterial chemotaxis. J. Biol. Chem. *266*, 8348–8354.

Lukat, G.S., McCleary, W.R., Stock, A.M., and Stock, J.B. (1992). Phosphorylation of bacterial response regulator proteins by low molecular weight phospho-donors. Proc. Natl. Acad. Sci. USA *89*, 718–722.

Lupas, A.N., and Stock, J. (1989). Phosphorylation of an N-terminal regulatory domain activates the CheB methylesterase in bacterial chemotaxis. J. Biol. Chem. *264*, 17337–17342.

Maddock, J.R., and Shapiro, L. (1993). Polar location of the chemoreceptor complex in the *Escherichia coli* cell. Science *259*, 1717–1723.

Marcus, S., Polverino, A., Barr, M., and Wigler, M. (1994). Complexes between STE5 and components of the pheromone-responsive mitogen-activated protein kinase module. Proc. Natl. Acad. Sci. USA *91*, 7762–7766.

McNally, D.F., and Matsumura, P. (1991). Bacterial chemotaxis signaling complexes: formation of a CheA/CheW complex enhances autophosphorylation and affinity for CheY. Proc. Natl. Acad. Sci. USA *88*, 6269–6273.

Milligan, D.L., and Koshland, D.E., Jr. (1988). Site-directed cross-linking: establishing the dimeric structure of the aspartate receptor of bacterial chemotaxis. J. Biol. Chem. *263*, 6268–6275.

Minton, A.P. (1981). Excluded volume as a determinant of macromolecular structure and reactivity. Biopolymers *20*, 2093–2120.

Mochly-Rosen, D. (1995). Localization of protein kinases by anchoring proteins: a theme in signal transduction. Science *268*, 247–251.

Nakayama, T., Wiest, D.L., Abraham, K.M., Munitz, T.I., Perlmutter, R.M., and Singer, A. (1993). Decreased signaling competence as a result of receptor overexpression: overexpression of CD4 reduces its ability to activate $p56^{lck}$ tyrosine expression and to regulate T-cell antigen receptor expression in immature $CD4^+CD8^+$ thymocytes. Proc. Natl. Acad. Sci. USA *90*, 10534–10538.

Ninfa, E.G., Stock, A., Mowbray, S., and Stock, J. (1991). Reconstitution of the bacterial chemotaxis signal transduction system from purified components. J. Biol. Chem. *266*, 9764–9770.

Northrup, S.H., and Erickson, H.P. (1992). Kinetics of protein-protein association explained by Brownian dynamics computer simulation. Proc. Natl. Acad. Sci. USA *89*, 3338–3342.

Parkinson, J.S. (1978). Complementation analysis and deletion mapping of *Escherichia coli* mutants defective in chemotaxis. J. Bacteriol. *135*, 45–53.

Pawson, T. (1995). Protein modules and signalling networks. Nature *373*, 573–580.

Pawson, T., and Schlessinger, J. (1993). SH2 and SH3 domains. Curr. Biol. *3*, 434–442.

Press, W.H., Teukolsky, S.A., Vetterling, W.T., and Flannery, B.P. (1992). Numerical Recipes in C, Cambridge, UK: Cambridge University Press.

Pruss, B.M., and Wolfe, A.J. (1994). Regulation of acetyl phosphate synthesis and degradation, and the control of flagellar expression in *Escherichia coli*. Mol. Microbiol. *12*, 973–984.

Sanders, D.A., Mendez, B., and Koshland, D.E., Jr. (1989). Role of CheW protein in bacterial chemotaxis: overexpression is equivalent to absence. J. Bacteriol. *171*, 6271–6278.

Schuster, S.C., Swanson, R.V., Alex, L.A., Bourret, R.B., and Simon, M.I. (1993). Assembly and function of a quaternary signal transduction complex monitored by surface plasmon resonance. Nature *365*, 343–346.

Stewart, R.C. (1993). Activating and inhibitory mutations in the regulatory domain of CheB, the methylesterase in bacterial chemotaxis. J. Biol. Chem. *266*, 1921–1930.

Stewart, R.C., Russell, C.B., Roth, A.F., and Dahlquist, F.W. (1988). Interaction of CheB with chemotaxis signal transduction compo-

nents in *Escherichia coli*: modulation of the methylesterase activity and effects on cell swimming behavior. Cold Spring Harbor Symp. Quant. Biol. *53*, 27–40.

Stock, A., Koshland, D.E., Jr., and Stock, J. (1985). Homologies between the *Salmonella typhimurium* CheY protein and proteins involved in the regulation of chemotaxis, membrane protein synthesis, and sporulation. Proc. Natl. Acad. Sci. USA *82*, 7989–7993.

Stock, J.B., Lukat, G.S., and Stock, A.M. (1991). Bacterial chemotaxis and the molecular logic of intracellular signal transduction networks. Annu. Rev. Biophys. Biophys. Chem. *20*, 109–136.

Swanson, R.V., Bourret, R.B., and Simon, M.I. (1993a). Intermolecular complementation of the kinase activity of CheA. Mol. Microbiol. *8*, 435–441.

Swanson, R.V., Schuster, S.C., and Simon, M.I. (1993b). Expression of CheA fragments which define domains encoding kinase, phosphotransfer, and CheY binding activities. Biochemistry *32*, 7917–7924.

Tawa, P., and Stewart, R.C. (1994). Kinetics of CheA autophosphorylation and dephosphorylation reactions. Biochemistry *33*, 7917–7924.

Welch, M., Oosawa, K., Aizawa, S.-I., and Eisenbach, M. (1993). Phosphorylation-dependent binding of a signaling molecule to the flagellar switch of bacteria. Proc. Natl. Acad. Sci. USA *90*, 8787–8791.

Welch, M., Oosawa, K., Aizawa, S.-I., and Eisenbach, M. (1994). Effects of phosphorylation, Mg^{++}, and conformation of the chemotaxis protein CheY on its binding to the flagellar switch protein FliM. Biochemistry *33*, 10470–10476.

Welch, P.J., and Wang, J.Y.J. (1995). Disruption of retinoblastoma protein function by coexpression of its C pocket fragment. Genes Dev. *9*, 31–46.

Wolfe, A.J., McNamara, B.P., and Stewart, R.C. (1994). The short form of CheA couples chemoreception to CheA phosphorylation. J. Bacteriol. *176*, 4483–4491.

Wylie, D., Stock, A., Wong, C.-Y., and Stock, J. (1988). Sensory transduction in bacterial chemotaxis involves phosphotransfer between Che proteins. Biochem. Biophys. Res. Comm. *151*, 891–896.

Zimmerman, S.B., and Minton, A.P. (1994). Macromolecular crowding: biochemical, biophysical and physiological consequences. Annu. Rev. Biophys. Struct. Biol. *22*, 27–65.

Zimmerman, S.B., and Trach, S.O. (1991). Estimation of macromolecular concentrations and excluded volume effects for the cytoplasm of *Escherichia coli*. J. Mol. Biol. *222*, 599–620.